

Experimental investigation on mechanical characterization of 3D printed PLA produced by fused deposition modeling (FDM)

Moradi, M., Aminzadeh, A., Rahmatabadi, D. & Hakimi, A.

Published PDF deposited in Coventry University's Repository

Original citation:

Moradi, M, Aminzadeh, A, Rahmatabadi, D & Hakimi, A 2021, 'Experimental investigation on mechanical characterization of 3D printed PLA produced by fused deposition modeling (FDM)', Materials Research Express, vol. 8, no. 3, 035304.

<https://dx.doi.org/10.1088/2053-1591/abe8f3>

DOI 10.1088/2053-1591/abe8f3

ESSN 2053-1591

Publisher: IOP Publishing

Original content from this work may be used under the terms of the Creative Commons Attribution 4.0 licence. Any further distribution of this work must maintain attribution to the author(s) and the title of the work, journal citation and DOI.

Materials Research Express



PAPER

OPEN ACCESS

RECEIVED

25 January 2021

REVISED

18 February 2021

ACCEPTED FOR PUBLICATION

23 February 2021

PUBLISHED

10 March 2021

Original content from this work may be used under the terms of the [Creative Commons Attribution 4.0 licence](#).

Any further distribution of this work must maintain attribution to the author(s) and the title of the work, journal citation and DOI.



Experimental investigation on mechanical characterization of 3D printed PLA produced by fused deposition modeling (FDM)

Mahmoud Moradi¹, Ahmad Aminzadeh³ , Davood Rahmatabadi⁴ and Alireza Hakimi²

¹ School of Mechanical, Aerospace and Automotive Engineering, Faculty of Engineering, Environment and Computing, Coventry University, Coventry, United Kingdom

² Department of Mechanical Engineering, Faculty of Engineering, Malayer University, Malayer, Iran

³ Department of Mathematics, Computer Science and Engineering, Université du Québec à Rimouski, Rimouski, Québec, Canada

⁴ School of Mechanical Engineering, College of Engineering, University of Tehran, Tehran, Iran

E-mail: d.rahmatabadi@ut.ac.ir

Keywords: fused deposition modeling, infill-pattern, poly-lactic-acid, tensile test, mechanical properties

Abstract

This study aims to systematically experimental investigate the influence of infill-patterns (IPs) on specific mechanical responses of parts fabricated by fused deposition modeling (FDM). A poly-lactic-acid (PLA) feedstock filament is utilized in the manufacturing process. Furthermore, six types of infill-patterns (deposition angle), namely full honeycomb, rectilinear, triangular, fast honeycomb, grid, and wiggle, are designed and printed. In order to determine the mechanical properties of manufactured parts, tensile tests are carried out. The mechanical properties such as extension, stress, elongation, energy, and Young's modulus are considered as objective functions. As a result, there is a direct correlation between mechanical properties and infill patterns. Thus, it is essential to select the best infill-pattern in terms of their applications, giving sufficient strength without overdoing time and cost. Based on the results, a triangular infill-pattern has a maximum value of ultimate tensile strength and E-module (15.4 and 534 MPa, respectively). On the other hand, the wiggle pattern is more flexible.

1. Introduction

In recent years, speed up manufacturing processes has been one of the main challenges among academic and industrial centers. In this regard, rapid prototyping (RP) technologies have emerged. The RP is a technique that accelerates the process of manufacturing on different scales [1, 2]. The RP is mainly conducted based on two approaches, namely 3D printing or additive manufacturing (AM), which have received increased attention across several disciplines. The AM is a computer control-based system in which different materials such as metallic and plastic parts are built layer by layer [3, 4]. To date, various types of AM have been developed and introduced, for instance, selective laser sintering (SLS) [5], selective laser melting (SLM) [6–8], and fused deposition modelling (FDM) [9]. Among them, the FDM is the most widely used technique due to its extraordinary properties such as being a clean process, easy to operate, having excellent accuracy and repeatability, and durable manufacturing and dimensionally stabilize. Recently, this method is considered a hot topic among several scholars, which consists of highlighting the FDM technique's properties, analytically and experimentally. According to the literature [10], the main subject in this field is investigating print parameters' effect on mechanical properties and using optimization methods to achieve better properties, however, good researches have been done in other fields such as numerical analysis [11, 12]. In fact, the strong impact of printing parameters on the properties of the final piece and the use of new geometric parameters such as infill patterns and raster angle is still the main topic related to the FDM process.

As an initial study, Hutmacher *et al* [13] investigated the mechanical characteristics of polycaprolactone (PCL) scaffolds fabricated by the FDM. Zein *et al* [14] modeled a novel scaffold architecture through the FDM was used and selected a honeycomb infill pattern for designing parts. In order to enhance the surface finish of parts manufactured via the FDM, Galantucci *et al* [15] conducted an experimental study. Kiendl and Gao [16] used three different raster

Table 1. The physical and mechanical properties of the poly-lactic-acid filament.

Property	Value
Full Name	Polylactic acid (PLA)
Melting Point	150 to 160 °C (302 to 320 °F)
Glass Transition	60 °C–65 °C
Injection Mold Temperature	178 to 240 °C (353 to 464 °F)
Density	1.210–1.430 g · cm ^{−3}
Chemical Formula	(C ₃ H ₄ O ₂) _n
Crystallinity	37%
Tensile Modulus	2.7–16 GPa

angles, and they showed that by using and selecting the raster angle, mechanical properties including strength, elongation, toughness, and even failure mechanism could be controlled. Magalhaes *et al* [17] used the tensile and bending tests in the FDM framework to estimate the stiffness and strength of a sandwich part. Mechanical properties of cellular lattice structures fabricated by the FDM were analyzed numerically by Karamooz *et al* [18]. The influence of the FDM parameters on the tensile properties of carbon-fiber-reinforced plastic composites has been studied by Ning *et al* [19]. An experimental investigation was performed by Durão *et al* [20] to optimize the FDM process parameters. They concluded that print speed and the number of contours play a crucial role in the FDM. Moradi *et al* [21] aimed to study the influence of the FDM process parameters on manufactured specimens. Besides, they tried to reduce build time and part weight in the FDM process.

Here, a systematic experimental analysis is designed and manufactured FDM parts to define the impact of various types of IPs on mechanical properties. One of the most critical parameters affecting this purpose is the infill-patterns. In fact, increasing mechanical properties of printed parts via the FDM play a crucial role in the field. The infill-pattern's shape can significantly affect the mechanical properties, print time, and cost of the obtained part [22]. Therefore, the focus is placed on comparing the mechanical properties of printed samples based on six types of IP. In the current study, comprehensively experimental investigation of IPs on specific mechanical responses of fused deposition modeling (FDM) based on feedstock filament of poly-lactic-acid (PLA) and Six types of infill-patterns (deposition angle), namely full honeycomb, rectilinear, triangular, fast honeycomb, grid, and wiggly are considered.

2. Experimental work

Basically, computer-aided design (CAD) models are designed using Solid work software and converted to the stereolithography (STL) formatted file. All of the specimens were printed by Sizan3N FDM 3D printer with PLA filament. The mechanical and physical properties of the PLA selected are listed in table 1. Regarding the software and printing configurations, the toolpath calculation (G-code) was made by simplify3D Slicer Printing parameters.

The design of experiments (DOE) is correlated with preparing an efficient mixture of experiments essential to reach comprehensive investigation, which is statistically meaningful. DOE is a scientific approach that allows researchers to understand the aspects of a process better and determine how inputs (factors) affect outputs (responses). In this study, DOEs can be divided into three main phases: planning, carrying out the tests, and analyzing the results. In this current study, DOEs procedure (Taguchi model) and optimization of primary tests are considered based on previous studies [21, 22]. Figure 1 shows the flowchart concept of this study.

- **The first stage (Design):** Applying computer-aided design (CAD) model and numerical simulation to achieve an optimum production based on chain value.
- **The second stage (Manufacturing):** Using the STL format file and convert it into the G-code file.
- **The third step (Testing):** Implementing a non-destructive test (NDT) as an inspection method to achieve a reliable specimen.

Figure 2 provides an overview of the experimental works, showing the FDM process's schematic, the IPs used, and finally, the printed samples after the tensile test. In order to ensure the printing quality of the specimens, the temperature of the building platform is controlled at around 60 °C, and the filament is heated to 220 °C during the printing process. All printing parameters presented in table 2 were considered constant for all samples with different patterns [21].

As mentioned, the main focus is placed on comparing the mechanical properties of printed samples based on six types of IPs is explained in table 3. One of the advantages and necessities of 3D printing is that the parts can be

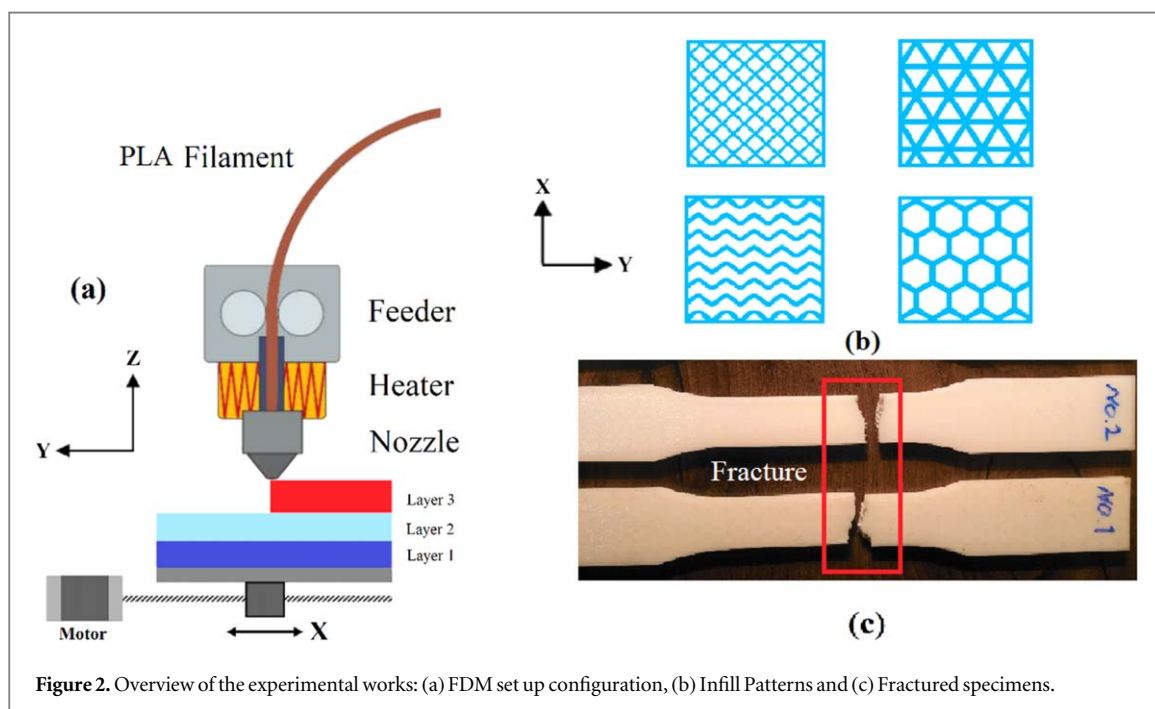
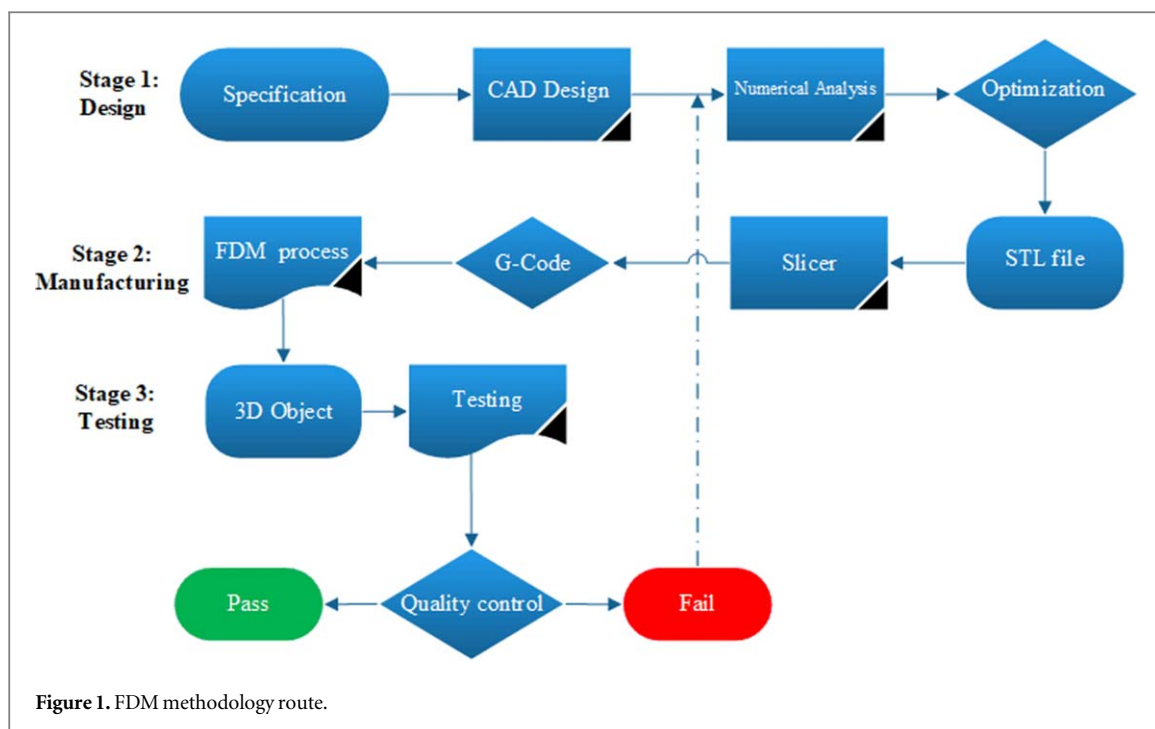
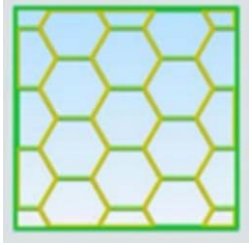

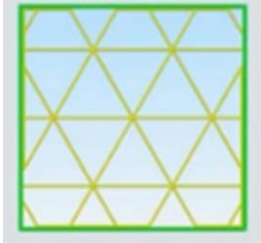
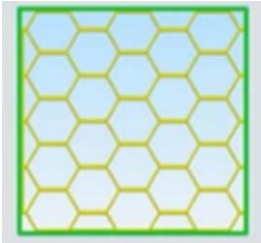




Table 2. The constant printing parameters.

Printing parameters (unit)	Value
Bed temperature (°C)	60
Nozzle Temperature (°C)	220
Printing speed (mm s ⁻¹)	20
Raster angle	45
Density (%)	50
Layer thickness (mm)	0.2
Overlap (%)	15%

Table 3. The infill-patterns for the FDM in this study.

Pattern	Structure	Explain
Full honeycomb		A bee panel or honeycomb infill is hexagonal geometry to fine distribution the load and wight based on the nature concept.
Rectilinear		A rectangular pattern is a logical structure in order to have a strong network in all directions.
Triangular		A triangular pattern is a typical structure in everyday life to reach extreme resistance in the direction of the walls.
Fast honeycomb		A fast honeycomb is greater than the rectangular pattern but with a longer printing time.
Grid		Grid is a self-explanatory 2D pattern to achieve an acceptable print speed.
Wiggle		This zigzag infill provides sufficient support and increases the rebound force.

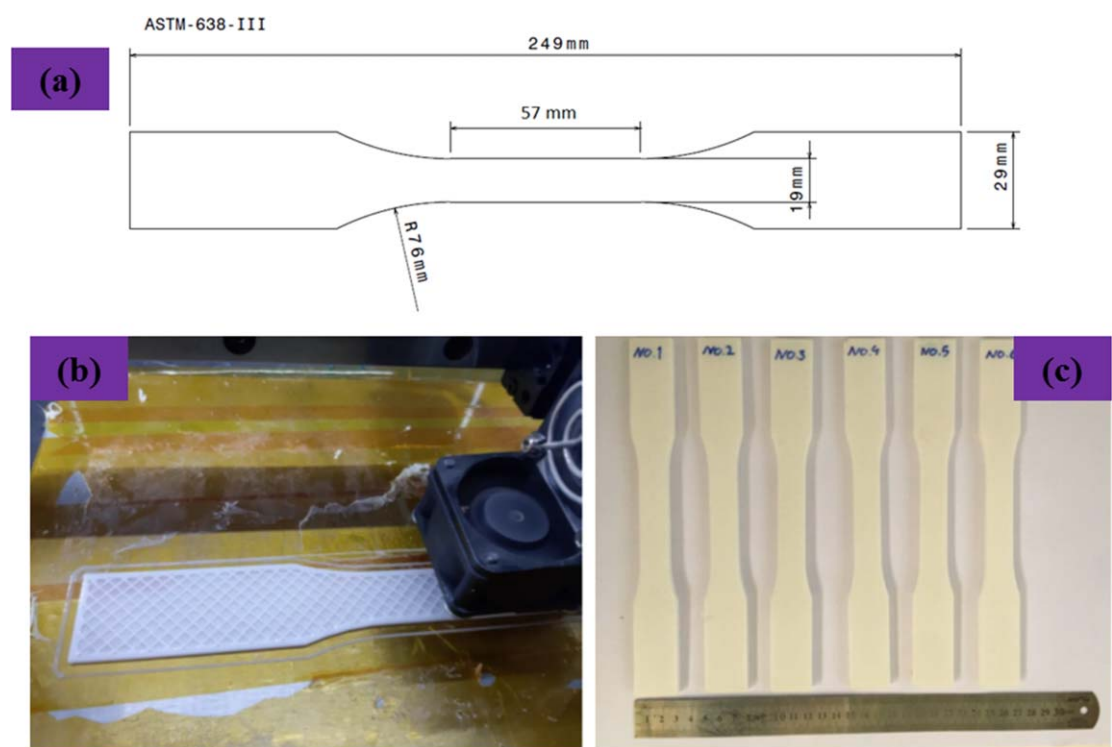


Figure 3. (a) Standard sample geometry for tensile test (b) producing the tensile test sample and (c) prepared specimen.

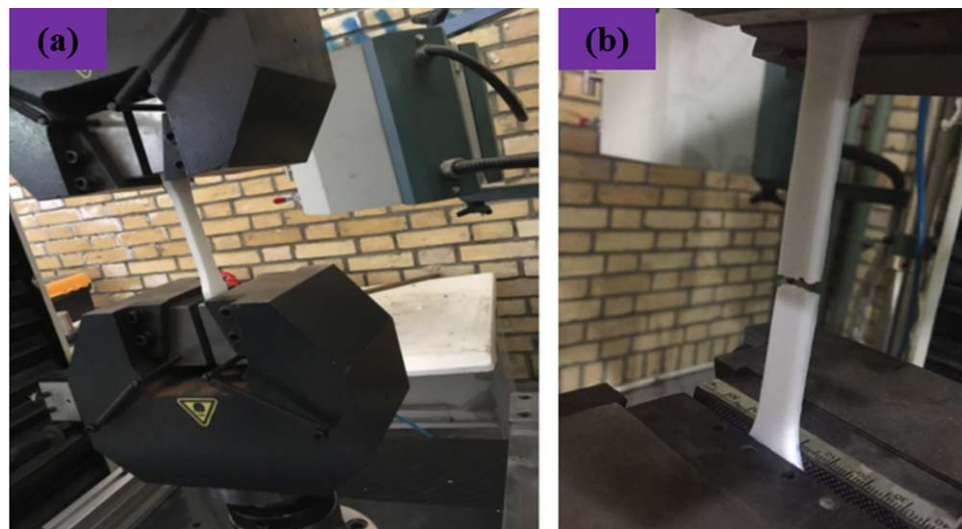


Figure 4. Uniaxial tensile test sample (a) during tensile test and (b) Fractured sample after tensile test.

hollow in different degrees. Regarding the production chain value, it not only reduces material consumption and cost but also optimizes the final weight and time management. Based on the literature, the most common types of IPs are selected as follows; full honeycomb, rectilinear, triangular, fast honeycomb, grid, and wiggly [23].

In order to define the mechanical properties of the printed materials, a uniaxial tensile test is applied to calculate key factors such as yield, ultimate force, extension, tensile strength, elongation, and absorbed energy for every 6 IPs with a Santam machine. According to figure 3(a), tensile specimens are printed based on ASTM D638 and the tensile test is repeated at least two times for each IPs to make sure the tests' accuracy. Tensile samples and printing procedure are shown in figures 3(b) and (c), respectively. The tensile speed is 0.1 mm/min, and the temperature is controlled at 23 °C. The tensile test machine and specimen during and after tensile test are presented in figure 4. Here, the effect of IPs on the mechanical properties is determined based on the fibers' print direction related to the loading direction and adhesion between the layers and fibers. There are two main methods to estimate build time that calculate by software packages, detailed analysis and parametric analysis.

Build time estimations tend to be specific to the system and material being used. In fact, build time is an essential factor in additive manufacturing costs; the details of build time are beyond this study's scope. It is worthwhile noting that the built time has been estimated through the use of a digital timer. As a result, due to the layering process incorporated, there is a direct correlation between the build time and the part height.

3. Result and discussion

At first, the observed sample's quality was checked and ensured the expected one and matched with the set parameters are presented in tables 2 and 3. Based on observation and special shape check method, there are no voids or surface cracks over the printed layer, and surface topography of all IPs specimen has clarified the achievement of good enough printing. Due to the varieties of available Additive Manufacturing (AM) technologies, one of the most critical points in cost-effective strategy is building time. However, for FDM, other factors are also involved, such as supports, fill density, contour and raster width, etc. In this section, full factorial mechanical properties and time conditions are shown in table 4. According to the results, the printing time of all produced samples with different IPs is in the range of 72 to 75 min and there is not much difference between them. Of course, the fast and full honeycomb have less and triangular IP has more printing time, respectively. The mechanical properties are then compared in three different sections (tensile strength, elongation and absorbed energy) for the maximum and the fracture points. The triangular and grid IPs are demonstrated the maximum and minimum tensile strength, respectively. On the other hand, wiggle has the highest elongation and absorbed energy values.

Firstly, tensile strength results and Young's modulus for every six IPs are compared with each other and are summarized in figures 5–9. From these figures, it is seen that the amount of tensile force, strength, elongation, absorbed energy and Young's modulus experienced by printed samples has a significant dependency on infill-pattern. Generally, according to figure 5, the strength properties of the triangular and grid patterns are the highest and lowest, respectively. The grid and triangular are the most used pattern [24]. Grid pattern has the most significant advantage over other patterns is its simplicity and less time.

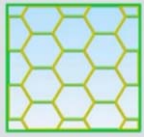

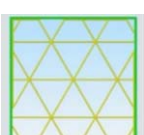
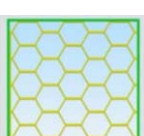


Moreover, triangular is a two-dimensional grid made of triangles, while a vertical force is applied to the surface of the object, this pattern shows high resistance and strength. This pattern is also suitable for thin rectangular pieces because there is little contact between these objects' walls. According to figure 5, the geometry of triangular resembles a truss with a continuous structural element. This structure leads to a homogenous distribution of stress in FDM samples. Because the distance between joint points in the grid pattern is long and a less infill density and much-trapped air, the grid infill-pattern resists the lowest value of the stress and force [25]. It is to be noted that for other patterns, this phenomenology is analogous [22, 26]. Here, the trapped air in different types of patterns is calculated and applied in design section (figure 6).

Regarding Young's modulus, every six IPs are compared in figure 7. Young's modulus and strength variations are almost identical, with the highest and lowest values being for triangular and full honeycomb, respectively. Of course, except for the triangular pattern, which is much higher than the others are, rectilinear and wiggle are close to each other (580.4 and 571.2 Mpa), and the last three patterns (full and fast honeycomb and grid) are not much different. Of course, the ratio of the maximum Young's modulus to the minimum is equal to 1.25, which indicates the relatively strong effect of the pattern on the elastic properties of the printed specimens.

Figure 8 reveals the elongation values for maximum elongation at UTS and total elongation at fracture point for each internal pattern. It could be concluded that wiggle pattern possesses the most considerable elongation and formability due to its flexible structure. Besides, the filaments in wiggle patterns are integrated and aligned, leading to a higher value of deformation. In this regard, the wiggle infill looks like wavy or zigzag lines, and aligning the filament strands with the applied force increases the ductility [14, 25]. In fact, in the same direction, changing the string's geometry from the wavy to the smooth with by applying force, the elongation and formability increases [27, 28]. This pattern is primarily used for flexible filaments such as softer nylon or other such rubbery filaments, where parts are designed for exceptional circumstances (twist, compress and rebound force). Moreover, this infill can still provide support to perpendicular walls.

Flexible productions in the field of engineering design and manufacturing refer to methods that can adapt when external changes occur. Some infill patterns lend themselves more to flexibility than others. The wiggle pattern resembles waves oriented in a single direction. Although every pattern has different advantages and disadvantages, the honeycomb pattern is the most practical and standard method in the 3D printing technique. In fact, the honeycomb pattern is an inspiring nature concept, which mainly in the construction of actual honeycombs. In this pattern, high infill promotes increased strength with diverse setting infill at a lower setting will also increase in a more flexible product. The honeycomb pattern strikes the perfect balance of strength and

Table 4. Mechanical properties response.

NO.	Pattern	Pattern shape	UTS (Mpa)	Elongation(%)	Energy (J)	Young's modulus (Mpa)	Build Time (minutes)
1	Full.honeycomb		15.397	2.8831	4788.343	534.043	72
2	Rectilinear		16.3196	2.812	4687.397	580.3556	73
3	Triangular		17.1489	2.5686	4554.239	667.636	75
4	Fasthoneycomb		14.6594	2.7059	4087.604	541.7569	72
5	Grid		14.3835	2.6576	3849.703	541.2214	74
6	Wiggle		15.582	2.7275	4323.943	571.2924	73

material use. Varying combinations of infill percentage and pattern can influence strength, material usage, and print times [29]. Overall, in order to improve the mechanical performance of a 3D printed part, it comes at the expense of print quality, speed, and affordability [30].

Energy absorption is another critical factor that is investigated in this study. In automotive structures, it is necessary to minimize the occurrence of damage caused by crash loads. Automobile manufacturers have applied various methods and systems to dissipate collision forces and decrease them by absorbing and redistributing them, which finally reduces their effects on the vehicle's occupants. The structures considered to have good energy absorption behavior used in the majority of transportation vehicles are the thin-walled (tubular) structures. Absorbed energy is defined as the surface below the load-displacement curve, which could be used to evaluate the toughness and the unanimity gained by the structures, especially in the automotive constructions during the frontal crash. The toughness study can also give us more accurate and useful information about the material's behavior because it includes both the parameters of strength and ductility. Therefore, the wiggle IP with lower strength has the highest absorbed energy toughness. According to figure 9, the fast honeycomb pattern and grid have the maximum and minimum absorbed energy, respectively.

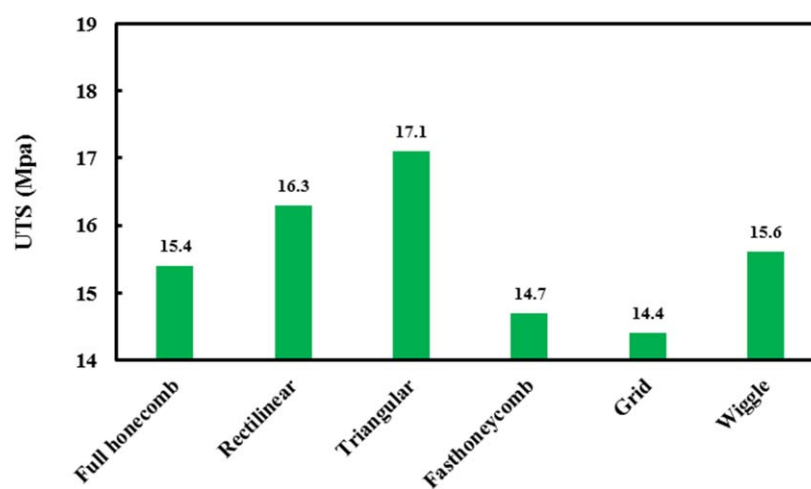


Figure 5. The influence of infill-pattern on the UTS.

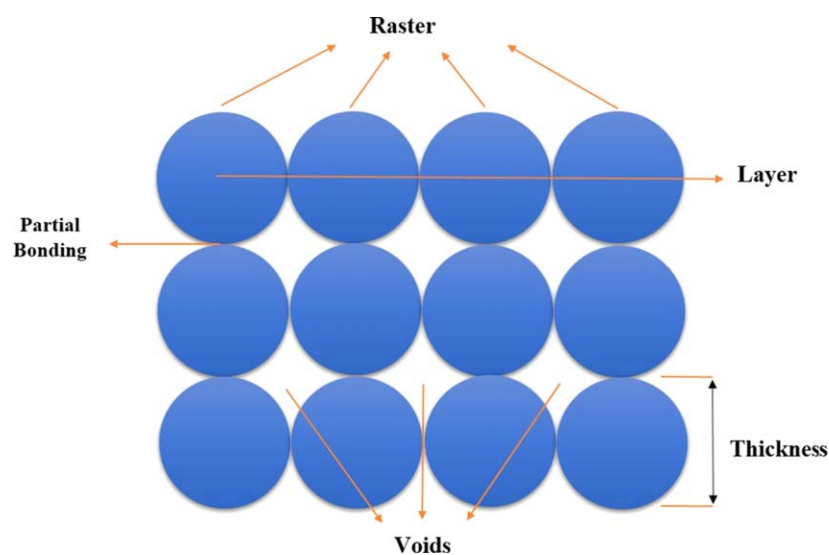


Figure 6. Interlayer bonding and trapped air using.

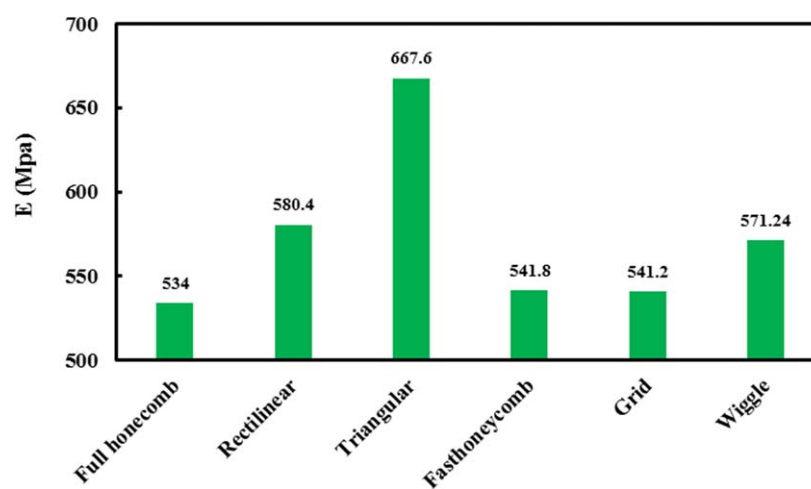
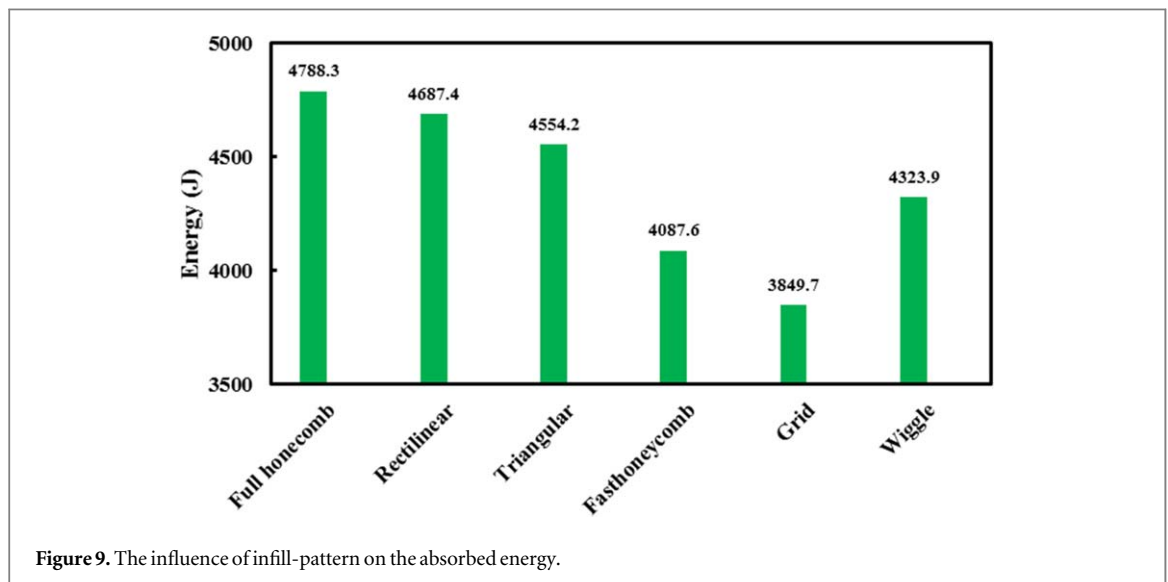
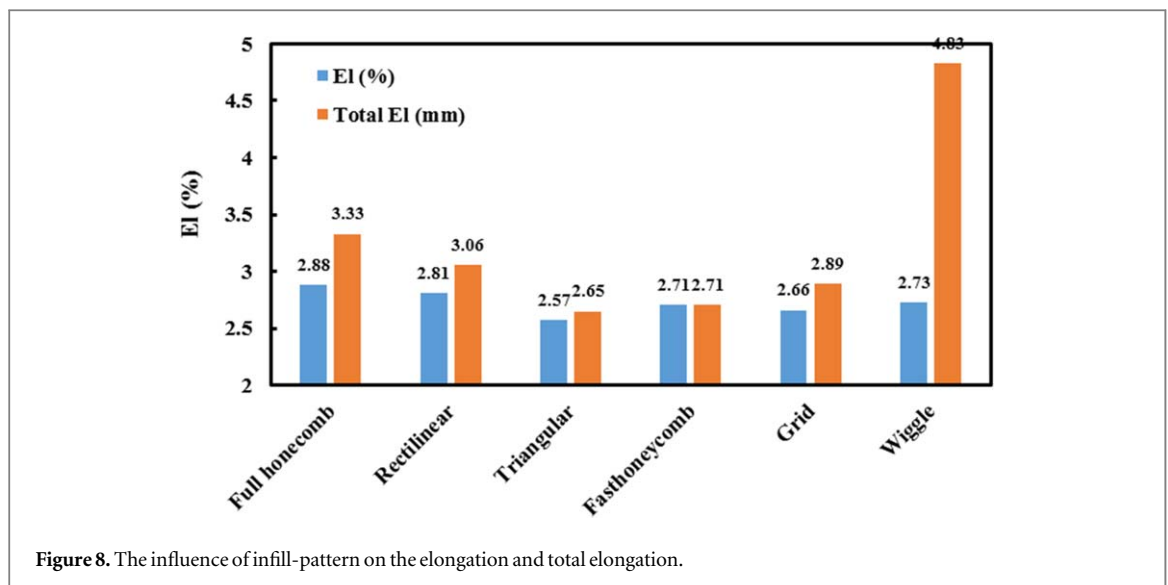


Figure 7. The influence of infill-pattern on the Young's modulus.



4. Conclusion

This paper investigates different types of infill-patterns (IPs) to accomplish fused deposition modeling (FDM) parts with respect to improving mechanical characteristics and the effect of IPs on the mechanical properties. The infill-patterns prepared were full honeycomb, rectilinear, triangular, fast honeycomb, grid, and wiggle. In addition, tensile strength, elongation, absorbed energy, and Young's modulus was defined as targets. An empirical setup was implemented, and tensile tests were conducted to calculate mechanical responses. This investigation concludes that:

In the triangular infill, due to the distance between joint points in the grid pattern is short. Subsequently, a less much-trapped air, the grid infill-pattern resists the highest value of the strength and Young's modulus and the maximum values of ultimate tensile strength were achieved for the triangular pattern. It is to be noted that for other patterns, this phenomenology is analogous.

Based on results, it could be concluded that wiggle pattern possesses the largest ductility and elongation due to its flexible structure. Overall, in order to improve the mechanical performance of a 3D printed part, it comes at the expense of print quality, speed and affordability. The best responses in elongation were obtained by wiggle pattern.

In terms of the absorbed energy as toughness evaluation, the wiggle pattern and fast honeycomb had the maximum and minimum absorbed energy, respectively.

The results show that the pattern has a significant effect on the mechanical properties of the PLA samples and different patterns can be used to achieve different good properties. For example, the triangle has the highest strength and Young's modulus, wiggle and fast honeycomb had the highest elongation and absorbed energy.

ORCID iDs

Ahmad Aminzadeh  <https://orcid.org/0000-0002-8312-8303>

Davood Rahmatabadi  <https://orcid.org/0000-0002-6898-3061>

References

- [1] Abdullah J and Hassan A Y 2005 Rapid prototyping in orthopaedics: principles and applications *Bone Grafts Bone Substitutes Basic Sci. Clin. Appl.* (World Scientific Publishing Co) pp 547–61
- [2] Upcraft S and Fletcher R 2003 The rapid prototyping technologies *Assem. Autom.* **23** 318–30
- [3] Gibson I, Rosen D, Stucker B, Gibson I and Rosen D 2015 *Stucker B. Extrusion-Based Systems. Addit. Manuf. Technol.* (New York: Springer) 147–73
- [4] Huang S H, Liu P, Mokasdar A and Hou L 2013 Additive manufacturing and its societal impact: a literature review *Int. J. Adv. Manuf. Technol.* **67** 1191–203
- [5] Delgado J, Serenó L, Monroy K and Ciurana J 2019 *Selective Laser Sintering. Mod. Manuf. Process.* (Hoboken, NJ: Wiley) 481–99
- [6] Yap C Y et al 2015 Review of selective laser melting: materials and applications *Appl. Phys. Rev.* **2** 041101
- [7] Zhang J, Song B, Wei Q, Bourell D and Shi Y 2019 A review of selective laser melting of aluminum alloys: processing, microstructure, property and developing trends *J. Mater. Sci. Technol.* **35** 270–84
- [8] Abedi H R, Hanzaki A Z, Azami M, Kahnooji M and Rahmatabadi D 2019 The high temperature flow behavior of additively manufactured Inconel 625 superalloy *Mater. Res. Express* **6** 116514
- [9] Boparai K S, Singh R and Singh H 2016 Development of rapid tooling using fused deposition modeling: a review *Rapid Prototyp J* **22** 281–99
- [10] Dave H K, Patel B H, Rajpurohit S R, Prajapati A R and Nedelcu D 2021 Effect of multi-infill patterns on tensile behavior of FDM printed parts *J Brazilian Soc Mech Sci Eng* **43** 1–15
- [11] Anoop M S, Senthil P and Sooraj V S 2021 An investigation on viscoelastic characteristics of 3D-printed FDM components using RVE numerical analysis *J Brazilian Soc Mech Sci Eng* **43** 1–13
- [12] Anoop M S and Senthil P 2019 Homogenisation of elastic properties in FDM components using microscale RVE numerical analysis *J Brazilian Soc Mech Sci Eng* **41** 1–16
- [13] Huttmacher D W, Schantz T, Zein I, Ng K W, Teoh S H and Tan K C 2001 Mechanical properties and cell cultural response of polycaprolactone scaffolds designed and fabricated via fused deposition modeling *J. Biomed. Mater. Res.* **55** 203–16
- [14] Zein I, Huttmacher D W, Tan K C and Teoh S H 2002 Fused deposition modeling of novel scaffold architectures for tissue engineering applications *Biomaterials* **23** 1169–85
- [15] Galantucci L M, Lavecchia F and Percoco G 2009 Experimental study aiming to enhance the surface finish of fused deposition modeled parts *CIRP Ann—Manuf Technol* **58** 189–92
- [16] Kiendl J and Gao C 2020 Controlling toughness and strength of FDM 3D-printed PLA components through the raster layout *Compos Part B Eng* **180** 107562
- [17] Magalhães L C, Volpato N and Luersen M A 2014 Evaluation of stiffness and strength in fused deposition sandwich specimens *J Brazilian Soc Mech Sci Eng* **36** 449–59
- [18] Karamooz Ravari M R, Kadkhodaei M, Badrossamay M and Rezaei R 2014 Numerical investigation on mechanical properties of cellular lattice structures fabricated by fused deposition modeling *Int. J. Mech. Sci.* **88** 154–61
- [19] Ning F, Cong W, Hu Y and Wang H 2017 Additive manufacturing of carbon fiber-reinforced plastic composites using fused deposition modeling: effects of process parameters on tensile properties *J. Compos. Mater.* **51** 451–62
- [20] Durão L F C S, Barkoczy R, Zancul E, Lee H L and Bonnard R 2019 Optimizing additive manufacturing parameters for the fused deposition modeling technology using a design of experiments *Prog Addit Manuf* **4** 291–313
- [21] Moradi M, Meiabadi S and Kaplan A 2019 3D printed parts with honeycomb internal pattern by fused deposition modelling: experimental characterization and production optimization *Met. Mater. Int.* **25** 1312–25
- [22] Terekhina S, Skorniyakov I, Tarasova T and Egorov S 2019 Effects of the infill density on the mechanical properties of nylon specimens made by filament fused fabrication *Technologies* **7** 57
- [23] Akhouni B and Behraves A H 2019 Effect of filling pattern on the tensile and flexural mechanical properties of FDM 3D printed products *Exp. Mech.* **59** 883–97
- [24] Ma Q, Rejab M, Kumar A P, Fu H, Kumar N M and Tang J 2020 Effect of infill pattern, density and material type of 3D printed cubic structure under quasi-static loading *Proc. Inst. Mech. Eng. Part C J. Mech. Eng. Sci.* **095440622097166**
- [25] Aloyaydi B, Sivasankaran S and Mustafa A 2020 Investigation of infill-patterns on mechanical response of 3D printed poly-lactic-acid *Polym. Test.* **87** 106557
- [26] Rahmatabadi D, Aminzadeh A, Aberoumand M and Moradi M *Mechanical Characterization of Fused Deposition Modeling (FDM) 3D Printed Parts* 1st edn (Switzerland: Springer International Publishing) (<https://doi.org/10.1007/978-3-030-68024-4>)
- [27] Popescu D, Zapciu A, Amza C, Baci F and Marinescu R 2018 FDM process parameters influence over the mechanical properties of polymer specimens: a review *Polym. Test.* **69** 157–66
- [28] Aminzadeh A, Aberoumand M, Rahmatabadi D and Moradi M 2021 Metaheuristic approaches for modeling and optimization of FDM process *Fused Depos. Model. Based 3D Print ed H K Dave and J P Davim* (Springer International Publishing) (<https://doi.org/10.1007/978-3-030-68024-4>)
- [29] Srinivasan R, Ruban W, Deepanraj A, Bhuvanesh R and Bhuvanesh T 2020 Effect on infill density on mechanical properties of PETG part fabricated by fused deposition modelling *Mater. Today Proc.* **27** 3–7
- [30] Solomon I J, Sevel P and Gunasekaran J 2020 A review on the various processing parameters in FDM *Mater. Today Proc.* **27** 1838–42